

Supporting Information

Design Rules for the Broad Application of Fast (< 1 s) Methylamine Vapor Based,
Hybrid Perovskite Post Deposition Treatments

Ting Zhao,^{1,‡} Spencer T. Williams,^{1, ‡} Chu-Chen Chueh,¹ Dane W. deQuilettes,² Po-Wei
Liang,¹ David S. Ginger,² and Alex K.-Y. Jen^{1,2,*}

¹Department of Materials Science and Engineering, University of Washington, Seattle, WA 98195, USA

²Department of Chemistry, University of Washington, Seattle, WA 98195, USA

‡ Ting Zhao and Spencer T. Williams contributed equally to this work

*Email: ajen@u.washington.edu

| | Voc (V) | Jsc (mA/cm ²) | FF | PCE (%) |
|---------|--------------------|---------------------------|--------------------|----------------------|
| Control | 0.62 (0.63 ± 0.06) | 11.23 (11.73 ± 1.64) | 0.47 (0.48 ± 0.01) | 3.27 (3.46 ± 0.30) |
| Treated | 0.85 (0.83 ± 0.02) | 17.59 (16.48 ± 1.17) | 0.81 (0.80 ± 0.01) | 12.08 (10.92 ± 0.81) |

Table S1: Photovoltaic performance values of the control and treated devices shown in Figure 2d (outside the parenthesis) and the average value with deviation calculated from 10 representative devices (inside the parenthesis).

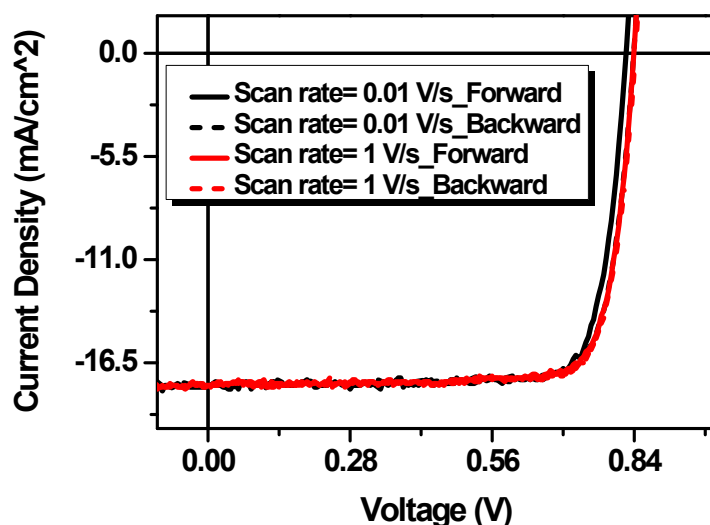


Figure S1: J-V measurements at different scan velocities and directions for MA⁰ vapor treated devices.

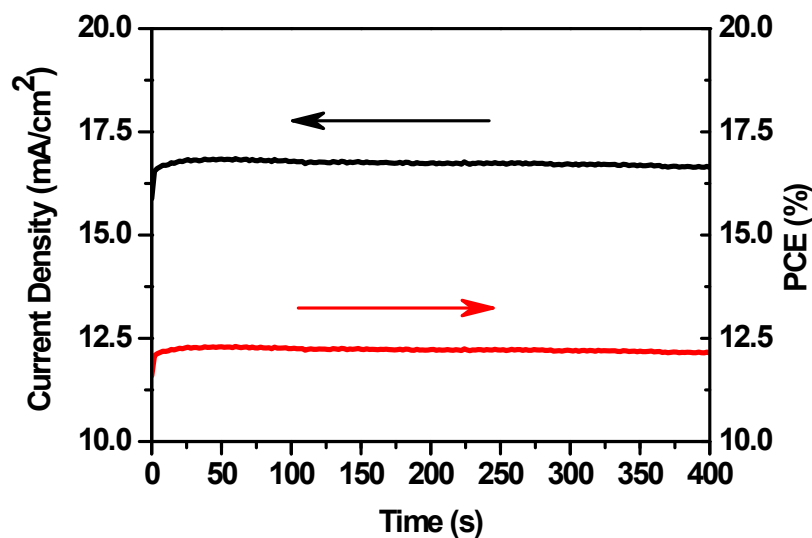


Figure S2: Steady-state current measured at a maximum power point (0.73 V) and stabilized power output.

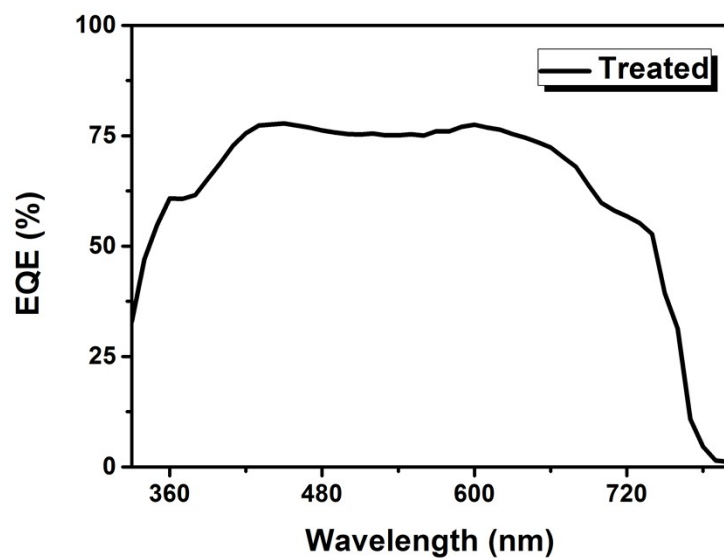


Figure S3: EQE spectra of treated perovskite solar cell. The calculated J_{sc} from the EQE spectra is 17.06 mA/cm^2 , which correspond well with the experimental J_{sc} 17.59 mA/cm^2 .

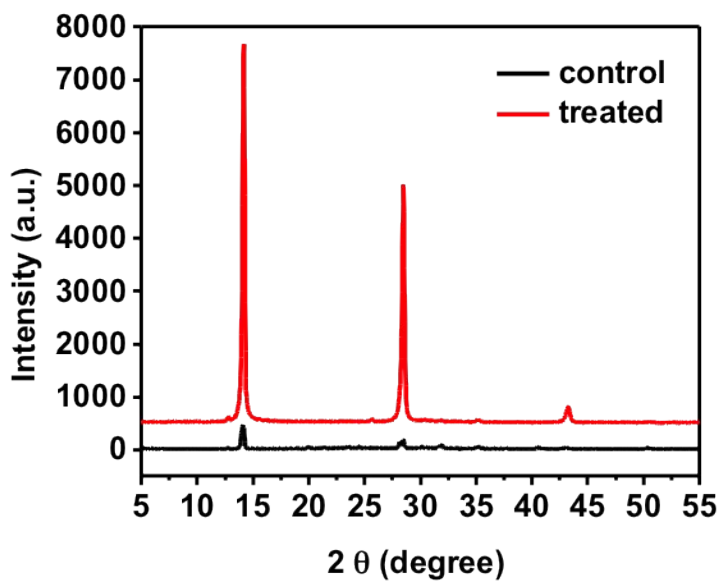


Figure S4: XRD patterns of MAPbI_3 film on glass before and after vapor treatment.

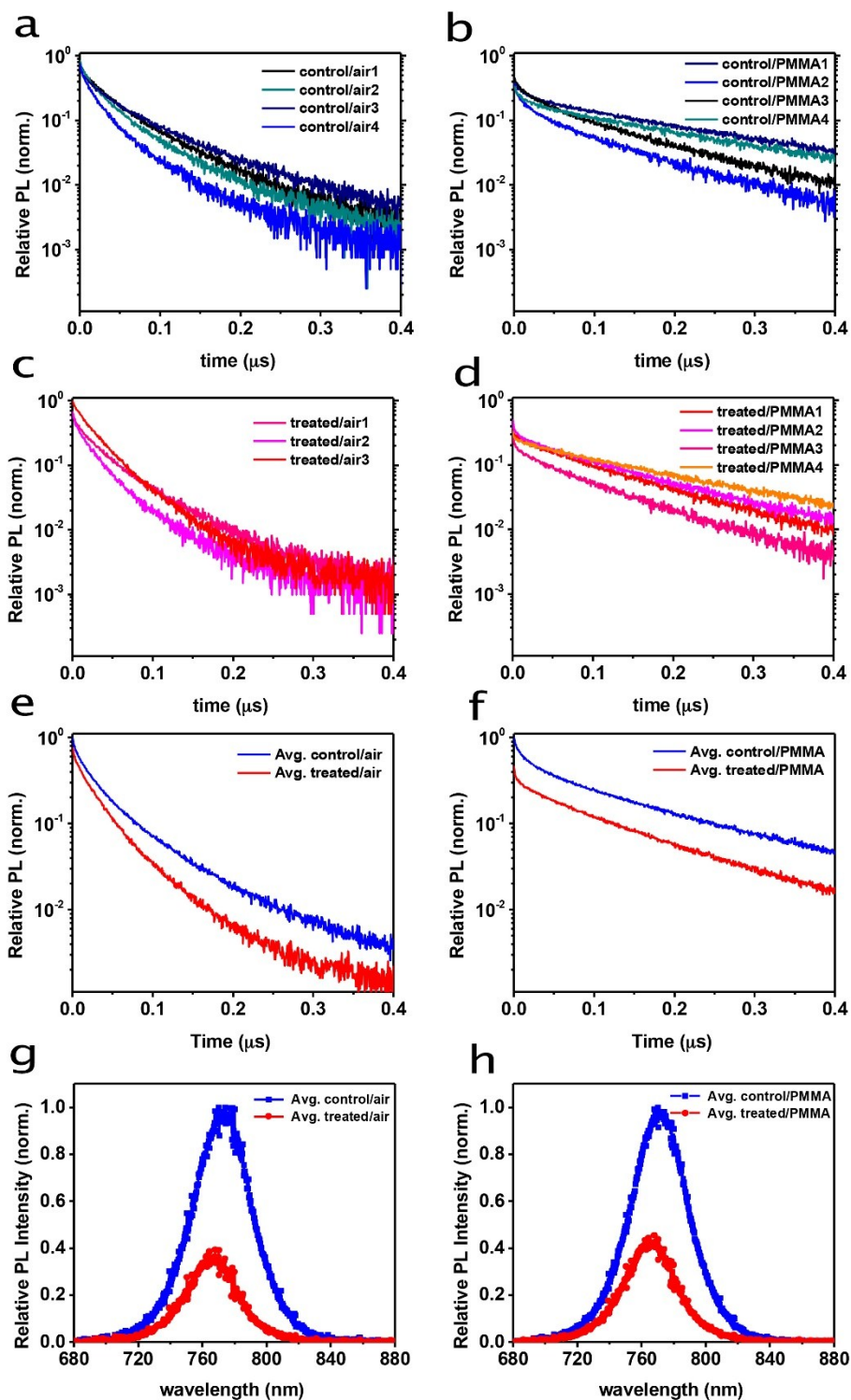


Figure S5: Several time-resolved PL decay curves of $\text{CH}_3\text{NH}_3\text{PbI}_3$ films on glass before treatment (a), before treatment with PMMA on top (b), after treatment (c), after treatment with PMMA on top (d), average PL decay of all traces with perovskite/air interface (e) and with perovskite/PMMA interface (f), average steady state PL spectra of all films with perovskite/air interface (g) and with perovskite/PMMA interface (h) showing consistent PL reduction after MA treatment across many samples.

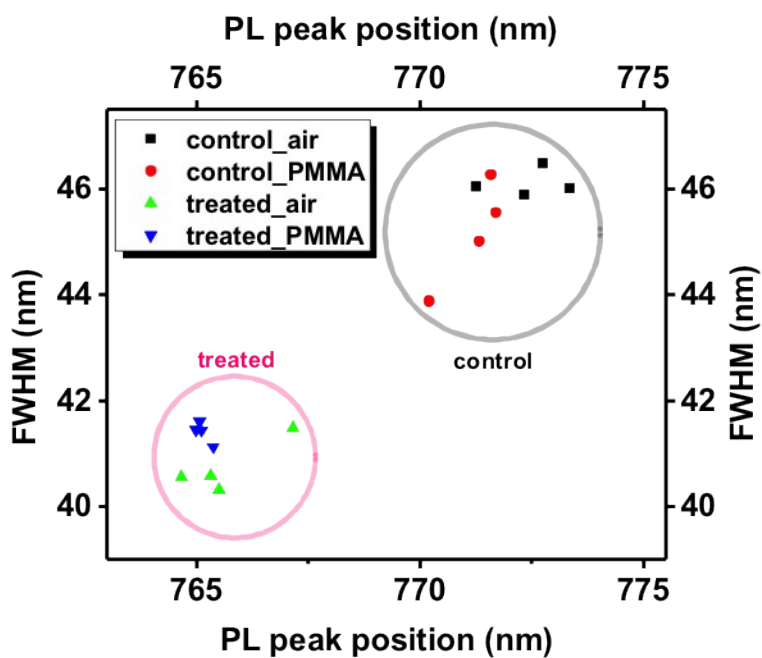


Figure S6: Gaussian fitting¹ of the steady state PL spectra yields a parameter plot of the PL peak position and full width half maximum (FWHM) of CH₃NH₃PbI₃ films on glass before treatment (black), before treatment with PMMA on top (red), after treatment (green), and after treatment with PMMA on top (blue).

Interpreting the dark field images: Dark field TEM is a technique that images the information contained within the diffracted electrons from a sample. Bright areas correlate with a region in the image that has the crystal structure and orientation to satisfy the Bragg condition. That means the objects that can be seen constitute the actual grain structure of the film (**Figure S6**). Where bright areas are arranged in close proximity with parallel, flat boundaries we have densely packed, highly oriented grain boundaries (region 3 in **Figure S6b**). Where we see many small bright areas clustered within areas that appear from SEM and bright field TEM as a single grain, we have difficulty to detect polycrystallinity (region 1 in **Figure S6b**). We are essentially seeing what satisfies the Bragg condition and thus areas within single grains that become dark are areas that violate this, specifically due to strain (bending) and internal defects (region 2 in **Figure S6b**). We use a circular objective aperture rather than an annular aperture for collecting this information which means that in any given dark field image we are only seeing a part of the total information contained in the sample's diffraction. In **Figure 5** and **S5**, we include one representative dark field image of each region taken in one quadrant of the sample's diffraction pattern. Specifically, the beam was tilted 0.675° off the optic-axis then rotated around the optic by 90° between each dark field exposure. Because of the size of our objective aperture ($\sim 10 \mu\text{m}$), this represents only part of the information contained within the dark field at that particular sample orientation. In general, most of the apparent grains do have some kind of diffracted signal but without an annular detector we can't represent the entirety of that information simultaneously.

The features we see in the dark field directly show us the size, shape, and nature of crystalline regions, but we can only see what satisfies the Bragg condition for diffraction so we can't see truly disordered regions or regions of a single crystal if it is highly strained or bent. This issue makes interpreting the dark field images for $\text{CH}_3\text{NH}_3\text{PbI}_3$ before vapor treatment challenging because strain and disorder are abundant. Many of the bright "stripes" that can be seen across larger domains are showing the region of that domain that is satisfying the Bragg condition. The actual grain size is larger than the bright region indicates as if the sample is tilted the bright region will move along the domain continuously. The complex microstructure buried within seemingly single crystalline grains from SEM further complicates the matter. Often the features we can see in dark field imaging manifest themselves in the bright field as is the case with the bending contrast in **Figure 1**.

After vapor exposure, microstructure in the dark field images becomes very simple and easy to interpret. Quantifying the change in grain size in this process would be misleading because it would direct the reader away from the most important aspect of the process which is a fundamental change in the nature of the grains, not just their size. As a top limit of grain size in the film before vapor treatment we can use SEM and bright field as an approximation. That said, microstructure within apparent grains and the disorder built into them makes this system distinct from the homogenous sea of crystallites after vapor treatment in more ways than an approximate grain size can communicate.

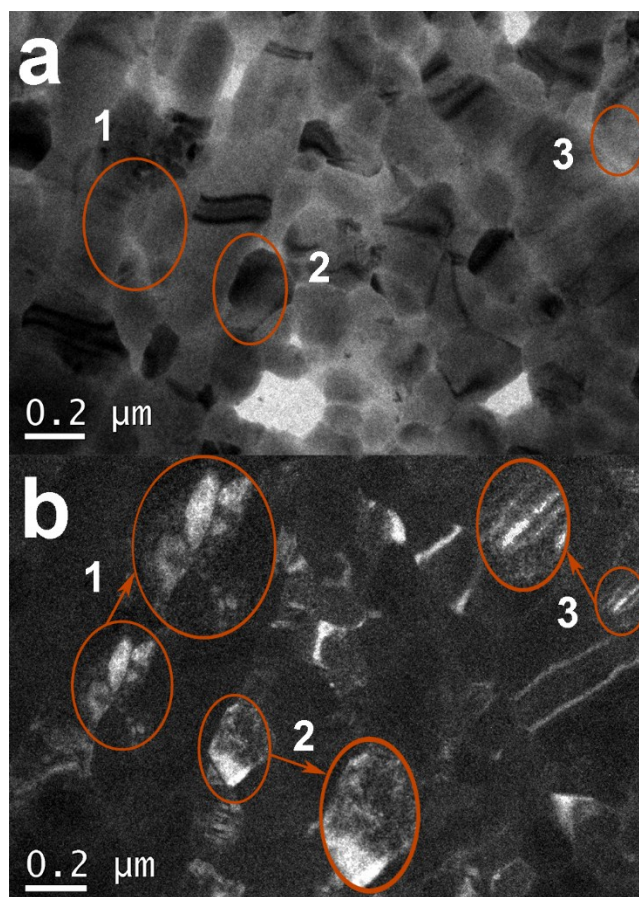


Figure S7: Bright- (a) and dark- (b) field TEM of a region before vapor treatment showing the microstructural complexity of MAPbI₃ grown by 1-step deposition. Regions that are highlighted show: (1) difficult to detect polycrystallinity, (2) highly strained and defective grains, and (3) dense and highly oriented grain boundaries. This technique cannot directly detect truly disordered domains.

Chemical sources of reactivity toward MA⁰ vapor: Sample Preparation and Microscopy Studies:

Sample Preparation:

MAPbBr₃: a 1M CH₃NH₃PbBr₃ precursor solution in DMF obtained by dissolving equimolar PbBr₂ (1M) and CH₃NH₃Br (1M) in DMF at 60°C and filtering through 0.45 μm PTFE filter was spin casted on top of PEDOT:PSS coated glass substrate at 6k rpm for 45s and then annealed at 100°C for 15 min. Vapor treatment was implemented as described in the Vapor Treatment Process part.

MASnI₃: a 1M CH₃NH₃SnI₃ precursor solution in DMF obtained by dissolving equimolar SnI₂ (1M) and CH₃NH₃I (1M) in DMF at 60°C and filtering through 0.45 μm PTFE filter was spin casted on top of PEDOT:PSS coated glass substrate at 6k rpm for 45s and then annealed at 100°C for 15 min. Vapor treatment was implemented as described in the Vapor Treatment Process part.

FAPbI₃: a 1M CH₃(NH₂)₂PbI₃ precursor solution in DMF obtained by dissolving equimolar PbI₂ (1M) and CH₃(NH₂)₂I (1M) in DMF at 60°C and filtering through 0.45 μm PTFE filter was spin casted on top of PEDOT:PSS coated glass substrate at 6k rpm for 45s and then annealed at 170°C for 15 min. Vapor treatment was implemented as described in the Vapor Treatment Process part.

CsPbI₃: a 0.6M CsPbI₃ precursor solution in DMF obtained by dissolving equimolar PbI₂ (0.6M) and CsI (0.6M) in DMF at 60°C and filtering through 0.45μm PTFE filter was spin casted on top of PEDOT:PSS coated glass substrate at 6k rpm for 45s and then annealed at 100°C for 15 min. Vapor treatment was implemented as described in the Vapor Treatment Process part.

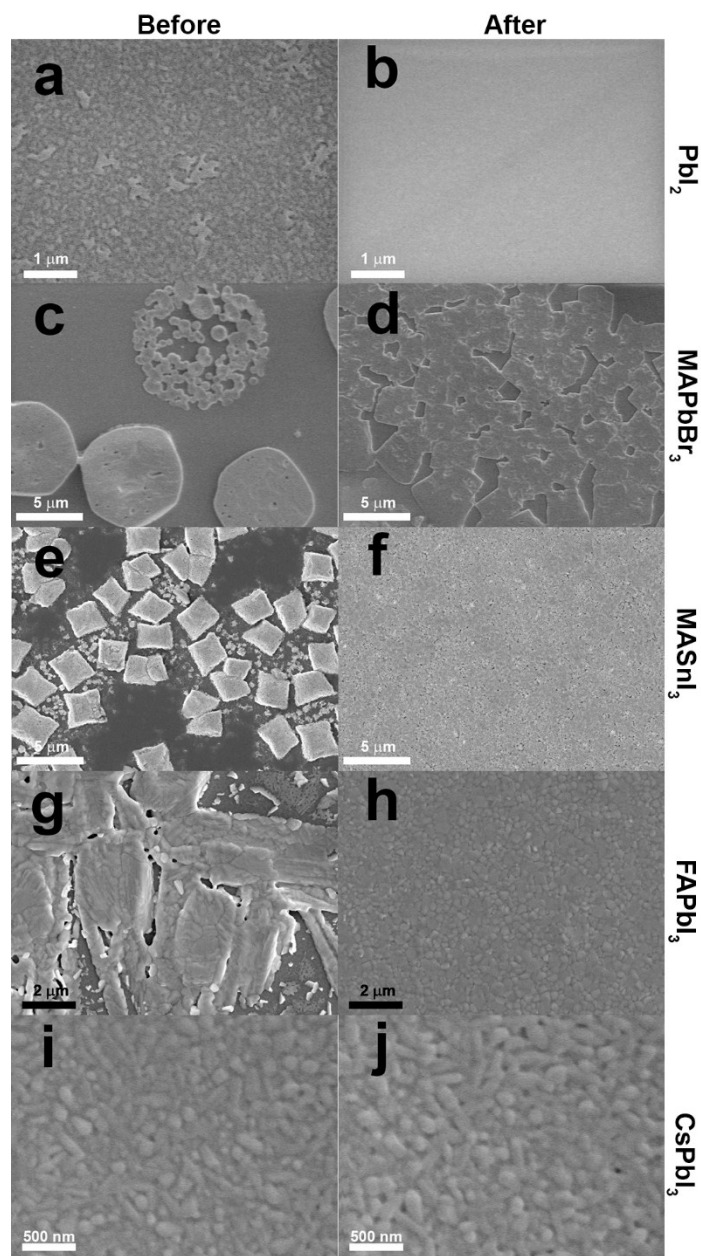


Figure S8: These SEM images show the effects of MA⁰ vapor treatment on (a)-(b) PbI₂, (c)-(d) MAPbBr₃, (e)-(f) MASnI₃, (g)-(h) FAPbI₃, and (i)-(j) CsPbI₃ at scales necessary to see relevant microstructural detail.

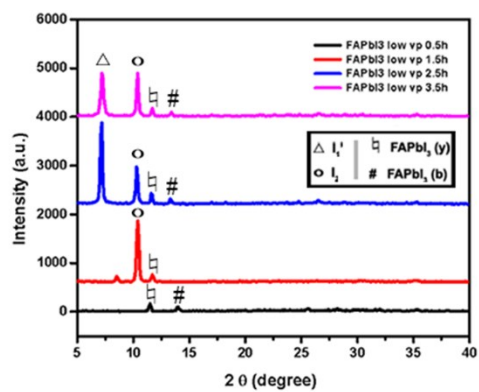


Figure S9: XRD showing the phase evolution of FAPbI₃ during low [MA⁰] treatment as a function of time. Phases indicated are listed in the inset legend with FAPbI₃ (y) and FAPbI₃ (b) indicating the yellow and black polymorphs respectively.

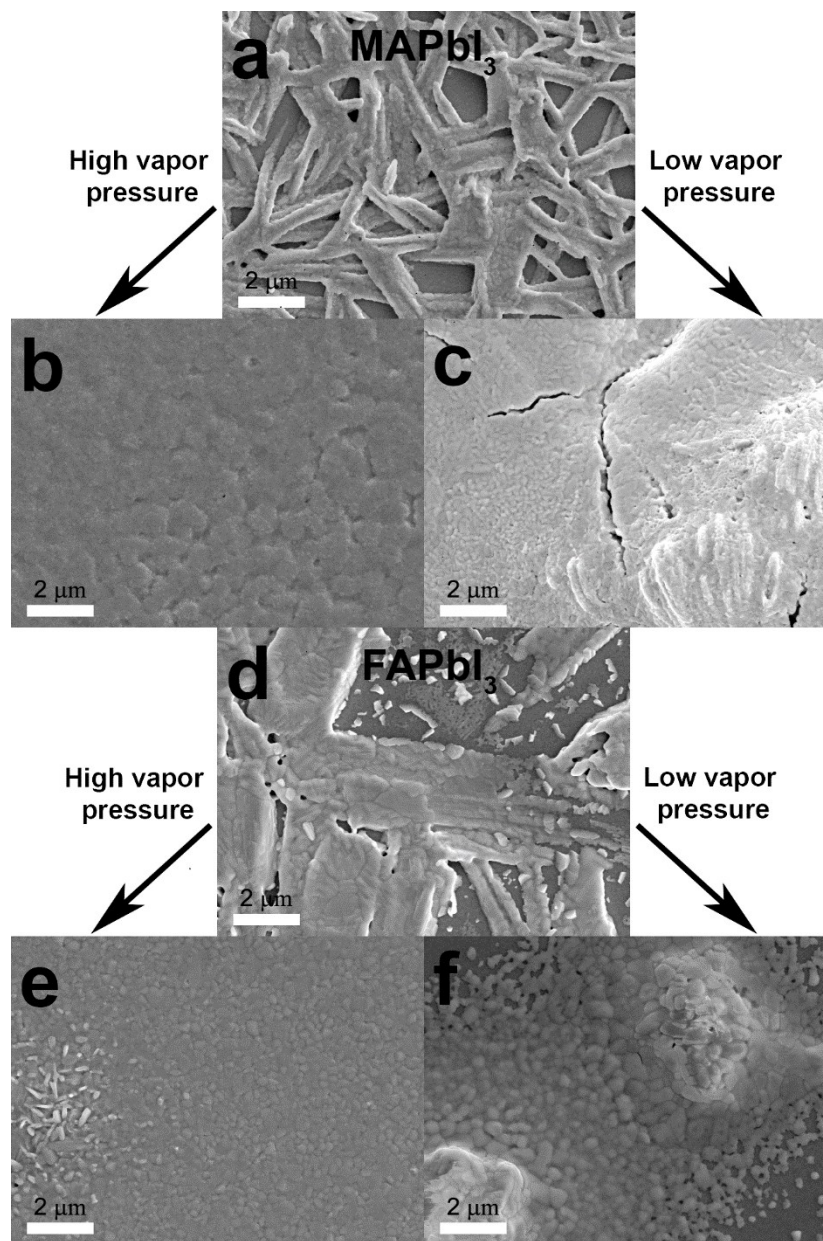


Figure S10: SEM of (a-c) MAPbI_3 and (d-f) FAPbI_3 before and after high and low $[\text{MA}^0]$ treatments. These are the same regions imaged in **Figure 4** of the main text.

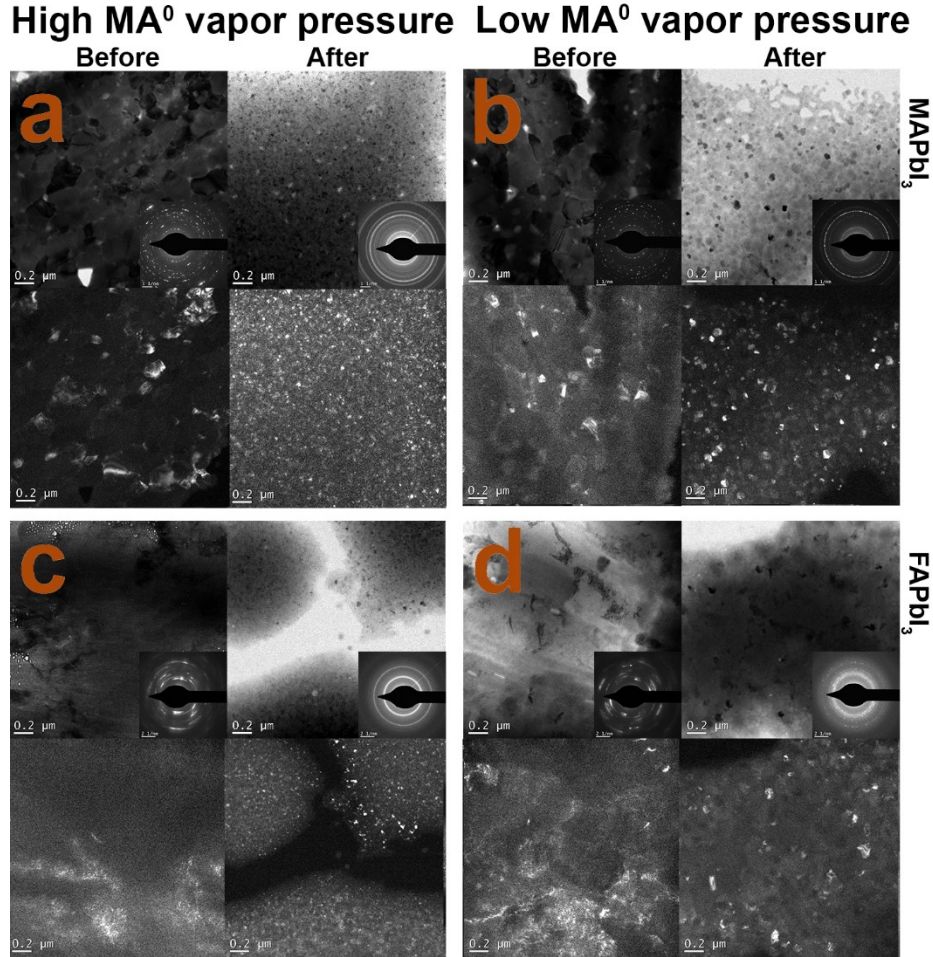


Figure S11: Each pane compared an identical region before and after MA⁰ vapor exposure with bright field imaging (top), select area electron diffraction (inset), and dark field imaging (bottom) with transmission electron microscopy of (a-b) MAPbI₃ and (c-d) FAPbI₃ for both (a & c) high and (b & d) low [MA⁰] treatments. These are the same regions imaged in **Figure 5** in the main text.

Low Vapor Treatment Process:

To avoid moisture, all processes were conducted in an N₂ filled glove box. Pure CH₃NH₃PbI₃ films were obtained through the procedure described in Vapor Treatment Process section at the beginning of the supporting information. For low MA⁰ vapor pressure exposure, perovskite films were put into a plastic petri dish (35mm x 10mm) and capped. A BT Barrier Pipette Tips box (15cm x 10cm x 10cm) was used to hold capped, 20mL vials, one of which contained 6 mL of 33wt% MA⁰ in ethanol without any internal or external gasket in the cap to allow a slow leak of vapor. The petri dish with perovskite films was placed atop this vapor source. The lower density of amine vapor compared to N₂ facilitated exposure with this chamber geometry. The box was sealed by three layers 3M 88 Electrical Tape to slow vapor leakage. A rough diagram of the system is offered in **Figure S11** for clarity.

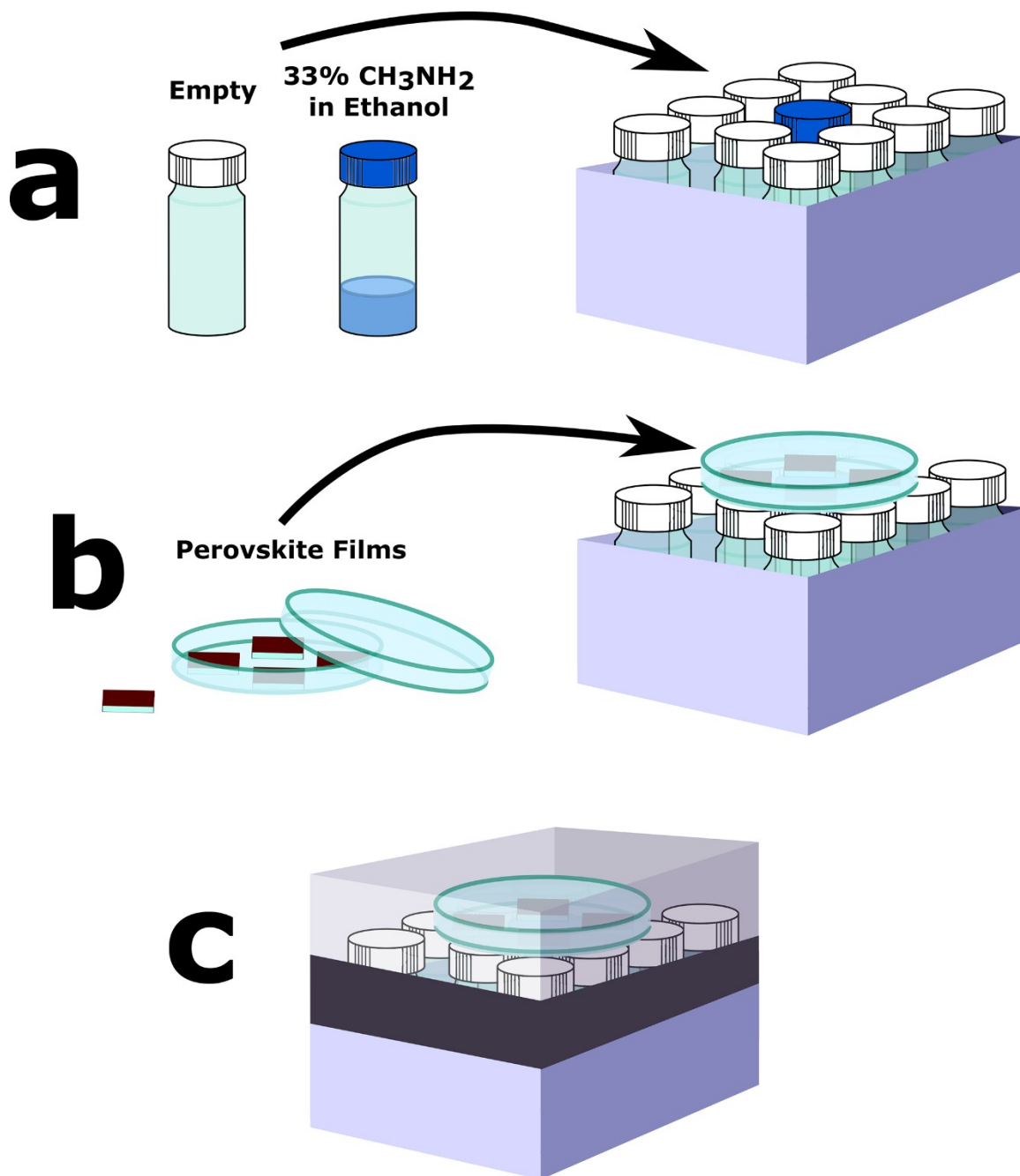


Figure S12: Schematic outline of the low MA⁰ vapor treatment process illustrating: a) inserting capped, 20 ml vials, one with methylamine solution in the center and empty vials around it for support; b) placing perovskite films in a closed petri dish resting on the vials, centered on the vapor source; c) sealing of the chamber.

References

- (1) Wehrenfennig, C.; Liu, M.; Snaith, H. J.; Johnston, M. B.; Herz, L. M. Homogeneous Emission Line Broadening in the Organo Lead Halide Perovskite CH₃NH₃PbI₃-XClX. *J. Phys. Chem. Lett.* **2014**, *5*, 1300–1306.